The 2015 World Congress on
Advances in Structural Engineering and Mechanics (ASEM15)
Incheon, Korea, August 25-29, 2015

Design of integral abutment bridges for combined thermal and seismic loads

* Narges Easazadeh Far [1)], Shervin Maleki[2)], Majid Barghian[3)]

[1)]*Department of Structural Engineering, Seraj Higher Education institute, Tabriz, Iran*
[2)]*Department of Civil Engineering, Sharif University of Technology, Azadi Ave., Tehran, Iran*
[3)]*Department of Civil Engineering, Tabriz University, Tabriz, Iran*
[1)] E-mail: easazadehfar@tabrizu.ac.ir
[2)] E-mail:smaleki@sharif.edu
[3)] E-mail: barghian@tabrizu.ac.ir

Abstract. Integral abutment bridges have many advantages over bridges with expansion joints in terms of economy and maintenance costs. However, in the design of abutments of integral bridges temperature loads play a crucial role. In addition, seismic loads are readily transferred to the substructure and affect the design of these components significantly. Currently, the European and American bridge design codes consider these two load cases separately in their recommended design load combinations. In this paper, the importance and necessity of combining the thermal and seismic loads is investigated for integral bridges. A 2D finite element combined pile-soil-structure interactive model is used in this evaluation. Nonlinear behavior is assumed for near field soil behind the abutments. The soil around the piles is modeled by nonlinear springs based on p-y curves. The uniform temperature changes occurring at the time of some significant earthquakes around the world are gathered and applied simultaneously with the corresponding earthquake time history ground motions. By comparing the results of these analyses to prescribed AASHTO LRFD load combinations it is observed that pile forces and abutment stresses are affected by this new load combination. This effect is more severe for contraction mode which is caused by negative uniform temperature changes.

Keywords: Integral Bridge, nonlinear model, seismic load, thermal load, soil-structure interaction.

1. Introduction

An Integral abutment bridge (IAB) is composed of a continuous deck connected rigidly to abutments, thereby eliminating the expansion joints. The maintenance costs associated with the expansion joints and bearings of jointed bridges has led to increasing use of the IABs throughout the world–especially, in the USA, Canada, UK and South Korea, where integral bridges are becoming a design choice for short and moderate spans. These bridges are subjected to primary loads (live loads, dead loads, seismic loads, etc.) and secondary effects (shrinkage, creep, passive pressure, uniform

* Corresponding author, Ph.D., E-mail: easazadehfar@tabrizu.ac.ir
[1)] Ph.D.
[2)] Professor
[3)] Assoc. Professor

temperature changes, thermal gradients, etc.). Among these loads, uniform thermal and seismic loads play a major role in the response of IABs. Integral bridge abutments are commonly supported on one row of steel H-piles to provide sufficient flexibility for accommodating longitudinal bridge movements due to thermal effects. These piles are greatly affected by both thermal and longitudinal seismic loads.

The behavior of IABs under thermal loading has been studied in several papers. Duncan JM and Arsoy S. (2003), Tsang NCM and England GL. (2002), Dicleli M and Albhaisi SM. (2004), Fennema JL. *et al.* (2005), Shah BR. (2007) and Kim W and Laman JA. (2010) have contributed to experimental and numerical aspects of IABs behavior under thermal loading in the past decade. Kim and Laman (2013) established IAB displacement and internal force statistics based on uncertain thermal loading using the Monte Carlo simulations. The established IAB displacement and internal force statistics in their research provide a basis for future reliability-based design criteria development. Later, Kim *et al*. (2014) developed new reliability-based limit states for IABs considering different abutment support conditions under thermal loading to ensure IABs achieve with the same level of safety as other bridges. Prestressed concrete girder bridges were considered in their study and were subjected to concrete time-dependent effects (creep and shrinkage), backfill pressure, temperature fluctuation and temperature gradient.

The seismic behavior of IABs has been studied extensively as well. Spyrakos and Loannidis (2003) investigated the behavior of post tensioned IABs with emphasis on soil-structure interaction. Tegos *et al.* (2005) proposed two different abutment configurations to improve seismic behavior of integral bridges. Frosch *et al*. (2009) and Itani A and Pekcan (2011) investigated the seismic behavior of IABs and developed design recommendations. Maleki and Mahjoubi (2010) introduced a 2D finite element model for seismic analysis of retaining walls and integral bridge abutments. Based on their research results, new seismic soil pressure distributions were proposed to replace the Mononobe-Okabe equations.

Due to the integrity of the IAB structure and complex soil-structure-pile interactions, thermal and seismic loads greatly affect the design of IABs. As indicated above, many researchers have studied the behavior of IABs under thermal or seismic loads, separately. However, no research was found to study the coupling effects of the two loadings. Moreover, according to some design codes such as, AASHTO LRFD (2010) and Eurocode (2008), combining the thermal and seismic loads is not necessary for the design of bridges. Knowing that the code specified load combinations are primarily for bridges with expansion joints and thermal loading affects mainly the longitudinal response of a bridge, the necessity of investigating the addition of thermal loads to the seismic load combination in the longitudinal direction for jointless bridges seems obvious.

In this paper, the combination of seismic and actual thermal loads at the time of an earthquake is considered in the analysis of typical IABs. The response of bridges is compared against the existing load combinations defined in AASHTO. It is shown that ignoring thermal and seismic load combination in some cases can be very unsafe for integral bridges.

Table1 Selected earthquakes and their properties

No	Earthquake	Date & Time	Station	M	T_{occur} (^oC)	Thermal loading, $\Delta T(^oC)$ (based on $T_C = 20\ ^oC$)	Scale Factor		
							AASHTO 2010 Site Class D	AASHTO 2010 Site Class A	AASHTO 2007
1	Palm Spring	1989/07/08 Time: 9:20 UTC	12149 Desert Hot Springs	6	34	14	1.578	1.142	1.0245
2	El Centro	1940/05/18 Time: 4:37 UTC	117 El Centro Array #9	7.1	16	- 4	2.109	1.526	1.369
3	San Fernando	1971/02/9 Time: 4:00 UTC	279 Pacoima Dam	6.6	6	- 14	0.785	0.568	0.509
4	Parkfield	1966/06/28 Time: 4:26 UTC	1014 Cholame #5	6.1	25	5	1.886	1.365	1.225
5	Loma Prieta	1989/10/18 Time: 00:05 UTC	57007 Corralitos	6.9	28.3	8.3	1.183	0.856	0.768
6	Northridge	1994/01/17 Time: 12:31 UTC	24514 Sylmar - Olive View Med FF	6.7	10	-10	0.782	0.566	0.508
7	Imperial Valley	1979/10/15 Time: 23:16 UTC	958 El Centro Array #8	6.5	30.6	10.6	1.547	1.119	1.004
8	Tabas	1978/09/16 Local Time: 19:05	9101 Tabas	7.4	30	10	1.002	0.725	0.65
9	Whittier	1987/10/01 Time: 14:42 UTC	709 Garvey Res. - Control Bldg	6	19	-1	1.33	0.962	0.863
10	Nahanni Canada	1985/12/23 Time: 5:48 UTC	6097 Site 1	6.8	-10	-30	0.774	0.56	0.503

2. Code specified thermal and seismic load combinations

When dead, live, thermal and earthquake loadings are present, AASHTO LRFD (2010) considers thermal loading in “Strength I” combination as:

$$\text{Strength I (S-1)} = \gamma_p \text{ (permanent loads)} + \gamma_{LL} \text{ (live loads)} + \gamma_T \Delta T$$

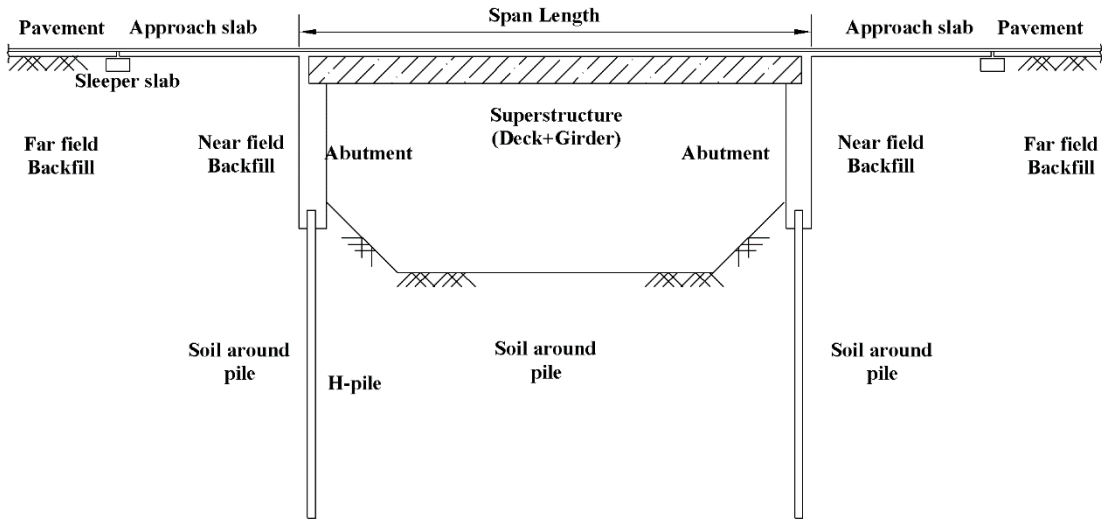

Fig. 1 Longitudinal section of the IAB

and considers earthquake loading in “Extreme Event I” combination as:

$$\text{Extreme Event I (EE-1)} = \gamma_p \text{ (permanent loads)} + \gamma_{EQ} \text{ (live loads)} + 1.0 \text{ EQ}$$

The load factors for dead, live and thermal loadings are given as: $\gamma_p = 1.25$, $\gamma_{LL} = 1.75$, $\gamma_{EQ} = 0.5$ and $\gamma_T = 0.5$. Herein, these two load combinations are designated as S-1 and EE-1 for simplicity.

In this paper, ΔT in S-1 load combination is calculated according to the procedure A of AASHTO for moderate climate and steel superstructure. This gives extreme temperature change of +30 ^{o}C expansion and -38 ^{o}C contractions for design purposes.

Thermal loading exists in IABs whenever the ambient temperature is not equal to the temperature at bridge construction time. This can exist during an earthquake as well. The average temperature at the time of earthquake occurrence (T_{occur}) of 10 significant earthquakes around the world is compiled and is shown in Table 1. Assuming the temperature at construction time of a bridge to be 20 ^{o}C (T_C= 20 ^{o}C), it is seen that some bridges experience expansion and some experience contraction at the time of earthquake. This is shown in the last column of the table. For an IAB without an expansion joint both of these modes can be critical and in combination with earthquake forces produce different results.

In order to study the significance of combined thermal and earthquake loading on IABs a new load combination (called EE+T) is considered which combines the actual thermal load present at the time of an earthquake and longitudinal earthquake loading as follows,

$$\text{EE+T} = \text{EE-1} + \Delta\text{Tactual} = \gamma_p \text{ (permanent loads)} + \gamma_{EQ}\text{(live loads)} + 1.0 \text{ EQ} + \Delta T_{actual}$$

From Table 1, it is seen that the actual temperature difference (ΔT_{actual}) ranges from +14 ^{o}C (Palm Spring) to -30 ^{o}C (Nahanni) based on a construction temperature of 20 ^{o}C.

Table 2 Steel sections properties

Section		Size	Height (cm)	Flange width (cm)	Flange thickness (cm)	Web thickness (cm)
Deck Girders		W 1000×975	111	43	9	5
Piles	Class D AASHTO 2010 analyses	H 300×300×10×15	30	30	1.5	1
	Class A AASHTO 2010 analyses	H 250×250×14×14	25	25.5	1.4	1.4
	AASHTO2007 analyses	H 250×250×9×14	25	25	1.4	0.9

In this paper, the EE+T load combination is applied to the IAB models and the results are compared to the code specified S-1 and EE-1 load combinations.

It will be shown that including the actual thermal load in some cases greatly affects the analyses results.

3. Finite element modeling

The 2D finite element structural models of single span integral bridges that are used in this study are described here. The superstructure of the bridge is composed of concrete slab with 20 cm thickness and steel beams at 2m spacing. The bridge cross-section and dimensions are shown in Fig.1. Two dimensional FE numerical models with an assumed width of 2 m (equal to deck beams spacing) are employed in this paper. Hence, the properties of the deck, abutment and soils are adjusted to reflect this width. Each abutment has 7m height and 1m wall thickness and is supported on a single row of steel H-piles with 12m length at 1m spacing. The steel sections for girders and piles are given in Table 2. To ensure a rigid connection between the pile and the concrete abutment, the piles are penetrated 50 cm inside the abutment. Weak axis of piles is perpendicular to the bridge longitudinal axis to provide sufficient flexibility. The deck is rigidly connected to the abutments. The material properties used in the bridge models are shown in Tables 3-5.

The abutment backfill is assumed to be a cohesionless soil with 30° angle of internal friction and a unit weight of 15.86 kN/m^3 at the top, increasing linearly to 16.72 kN/m^3 at the bottom of the wall. All soil properties are shown in Table 5.

Soil modeling follows the Maleki and Mahjoubi (2010) suggestion with nonlinear springs for near field soil and linear behavior for the free field soil. According to this model the near field soil behind the abutment is divided into layers and the following equation is used to estimate the shear modulus, *G*, at the middle of each layer:

$$G_Z = G_H \sqrt{\frac{z}{H}} \tag{1}$$

where G_z and G_H are the elastic shear modules at depths *z* and *H*, respectively.

Table 3 Properties of steel piles and Girders

Property	Value
Modulus of elasticity, *E* (GPa)	204
Poisson's ratio, *v*	0.3
Thermal expansion coefficient, *α* (1/^{o}C)	11.7×10^{-6}
Shear modulus, *G* (GPa)	78.4
Yield stress, F_y (MPa)	240
Ultimate stress, F_u (MPa)	370

Table 4 Properties of Concrete

Property	Value
Modulus of elasticity, *E* (GPa)	25.3
Poisson's ratio, v	0.2
Thermal expansion coefficient, *α* (1/^{o}C)	9.9×10^{-6}
Shear modulus, *G* (GPa)	10.5
Weight per unit volume, *γ* (kN/m^3)	24
compressive strength, f'_c (MPa)	28

Table 5 Properties of soils used in analyses

	Layer name	Depth, *z* (m)	Modulus of elasticity, *E* (MPa)	Shear modulus, *G* (MPa)	Weight per unit volume, *γ* (kN/m^3)	Poisson's ratio, *v*	Friction angle, *Φ*(^{o})
Near field soil	backfill	0-7	0-50	$19.23\sqrt{\frac{z}{7}}$	0. 1229z +15.86	0.3	30
Far field soil	1	0-2.25	22.19	8.53	16.42	0.3	34
	2	2.25-4.5	38.44	14.79	16.95	0.3	4
	3	4.5-7	50.18	19.3	17	0.3	34
Soils around piles	4	7-9.3	59.53	22.98	17.31	0.3	34
	5	9.3-11.6	67.64	26.02	17.56	0.3	34.5
	6	11.6-13.9	74.71	28.73	17.79	0.3	35
	7	13.9-16.2	81.18	31.22	18	0.3	35
	8	16.2-18.5	87.16	33.52	18.19	0.3	35

The equivalent springs representing soils adjacent to the abutment are modeled using nonlinear spring elements. The stiffness of each spring, defined as subgrade modulus, is derived as follows,

$$k_s = C_Z . \frac{G_Z}{H} \tag{2}$$

where C_Z is a constant representing the geometric properties of the model. The value of C_Z is assumed to be 1.35. This value is multiplied by tributary soil area of 1 m^2 to obtain the initial elastic linear stiffness of each spring.

Soil pressure varies from the at rest condition and is bounded by the active and passive soil pressures as follows:

$$K_a.\gamma.z \le \sigma_z \le K_p.\gamma.z \;\; \& \;\; \sigma_z = K_0.\gamma.z \;@\; \text{rest} \tag{3}$$

where

$$K_a = \frac{1-\sin\varphi}{1+\sin\varphi} \;\; , \;\; K_p = \frac{1+\sin\varphi}{1-\sin\varphi} \;\; , \;\; K_0 = 1-\sin\varphi \tag{4}$$

According to AASHTO (2010), all loads on the structure should be multiplied by a load factor. Hence, Eq. (3) is modified by multiplying the active pressure by a load factor of 1.5. The at-rest pressure is multiplied by a load factor of 1.35. The passive pressure is considered to be a resistance and requires no load factor.

Based on the above formulation, a nonlinear spring is defined in the finite element model to simulate the near field soil behavior. A typical force-displacement plot for this spring is shown in Fig. 2. In the actual model, this diagram must be shifted down to start at the origin. To compensate for this, a constant force of $1.35P_0$ is applied to the abutment at the same location.

The free field soil modeling consists of infinite half-space elastic layers of dense cohesion-less soil with properties shown in Table 5. This layer is free at the top and is considered to be pinned at the bottom and is also assumed to have a finite length equal to 4 times its height away from the wall. The free field soil layer is modeled using plane strain elements. Soil layers have different elastic properties; however, they are assumed to be constant within each layer.

Soil-pile interaction is modeled using nonlinear springs with stiffness varying according to p-y curves (Reese and Van Impe 2001). The soil-structure-pile model is shown in Fig. 3.

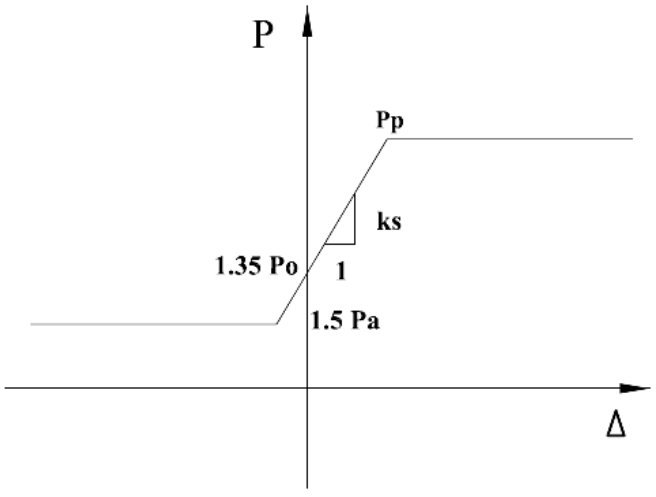

Fig.2 Factored force-displacement plot for the backfill springs

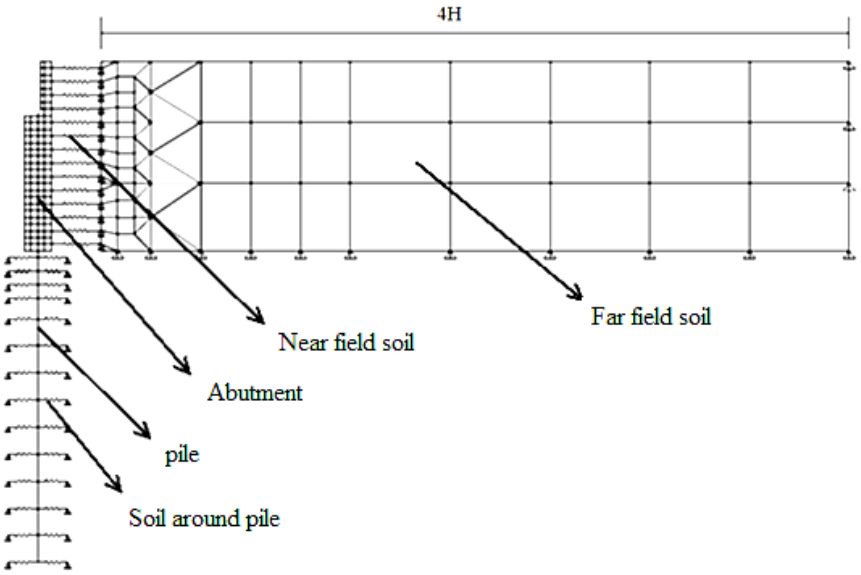

Fig.3 Soil-structure-pile model

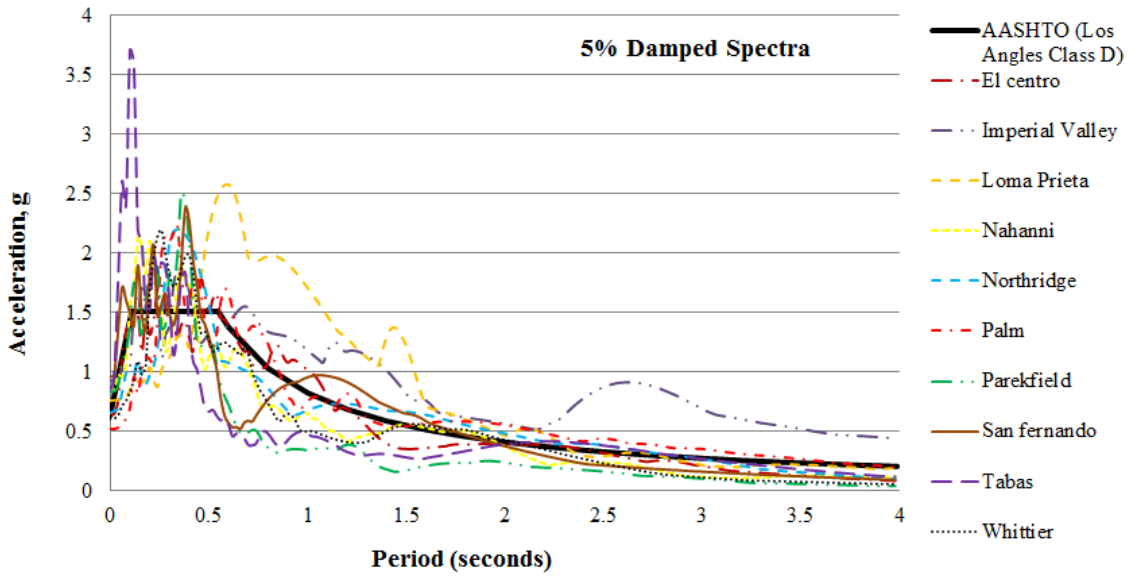

Fig. 4 Scaled records to AASHTO (2010) design spectrum with 5% damping for Los Angles-Class D

4. Analyses results

The results of nonlinear finite element dynamic time history analyses on the bridge models subjected to AASHTO's (2010) load combinations (S-1 & EE-1) and the proposed EE+T load combination are compared in this section. Span lengths of 20, 30, 40 and 50 m are considered. The deck's dead load is estimated at 6.3 kN/m^2. The live load considered is AASHTO's HL-93K truck loading. Seismic and thermal loadings are according to Table 1.

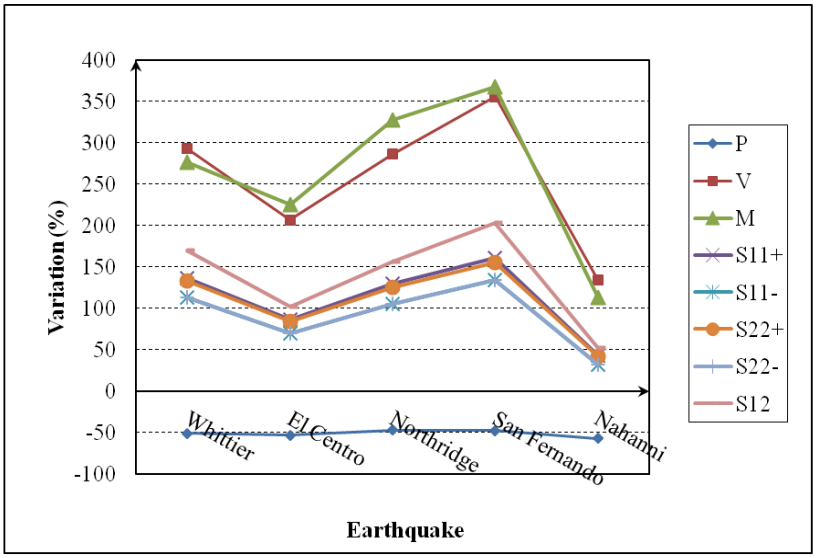

Fig. 5 Variation of pile internal forces and abutment stresses: proposed combination versus
AASHTO 2010 Strength I-contraction mode

Each earthquake time history is obtained from PEER (2013) for the specific location and is scaled to AASHTO's (2010) design response spectrum with 5% damping for Los Angles. The scaling applies to just longitudinal ground motion in the period range of 0.2T to 1.5T, where T is the main longitudinal period of the bridge. The scale factor for each earthquake is listed in Table 1 and the plot of scaled response spectra is shown Fig. 4. All bridges are assumed to have an 'Essential' operational classification and class 'D' site class unless otherwise noted.

Analyses results are given for internal forces of piles (axial force P, shear force V, and bending moment M) and abutment stresses (longitudinal normal stress S11, vertical normal stress S22 and shear stress S12) as obtained for S-1, EE-1 and EE+T load combinations.

4.1. Overall behavior

To see the overall IAB behavior under combined thermal and earthquake loading, the results for the 40 m span bridge is explored in detail first. The percentage of change in actions for the EE+T load combination as opposed to S-1 and EE-1 of AASHTO are plotted for each earthquake case and are shown in Figs. 5-8. Contraction and expansion modes (see Table 1) of earthquakes are plotted separately. Careful examination of Figs. 5-8 leads to the following conclusions:

a) For all earthquakes, comparing the load combination EE+T with S-1 of AASHTO indicates that significant changes (up to 350%) in actions exist. This is mainly due to earthquake forces present in EE+T case and not due to thermal forces. However, it shows that the S-1 (gravity+thermal) load combination cannot capture the temperature loading that accompanies an earthquake in a safe manner.

b) Comparing the EE+T with EE1 of AASHTO shows that the contraction mode (with negative ΔT) results more significant changes in actions than the expansion mode.
c) Comparing the EE+T with EE1 of AASHTO shows that the piles moments and shears are more affected than the other actions. A maximum change of near 8% is observed for these actions for Nahanni earthquake. This was of course to be expected as this earthquake had the highest actual ΔT of -30^{o}C.

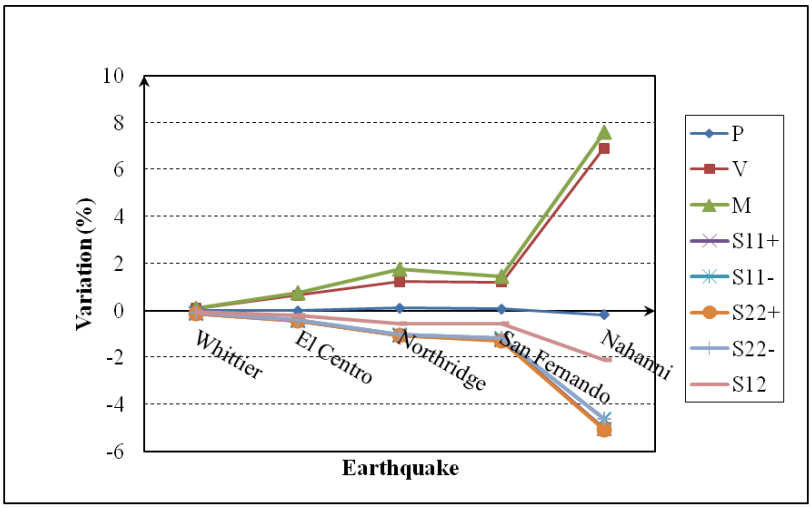

Fig. 6 Variation of pile internal forces and abutment stresses: proposed combination versus
AASHTO 2010 Extreme Event I-contraction mode

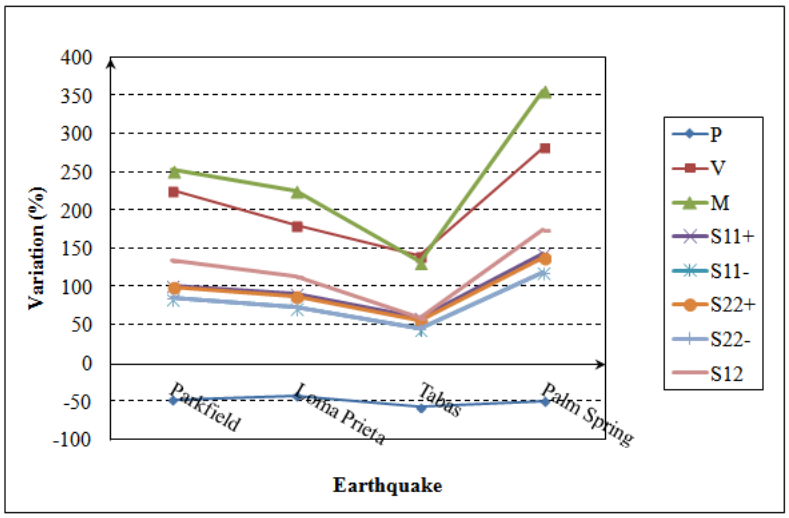

Fig. 7 Variation of pile internal forces and abutment stresses: proposed combination versus
AASHTO 2010 Strength I-expansion mode

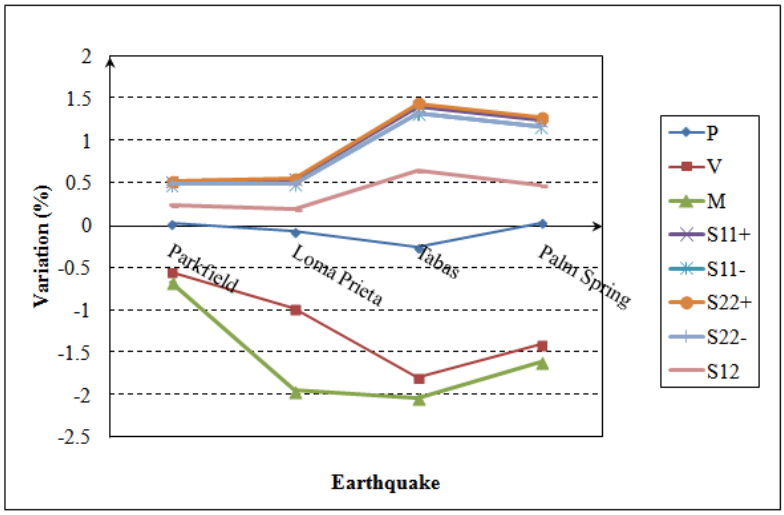

Fig. 8 Variation of pile internal forces and abutment stresses: proposed combination versus
AASHTO 2010 Extreme Event I-expansion mode

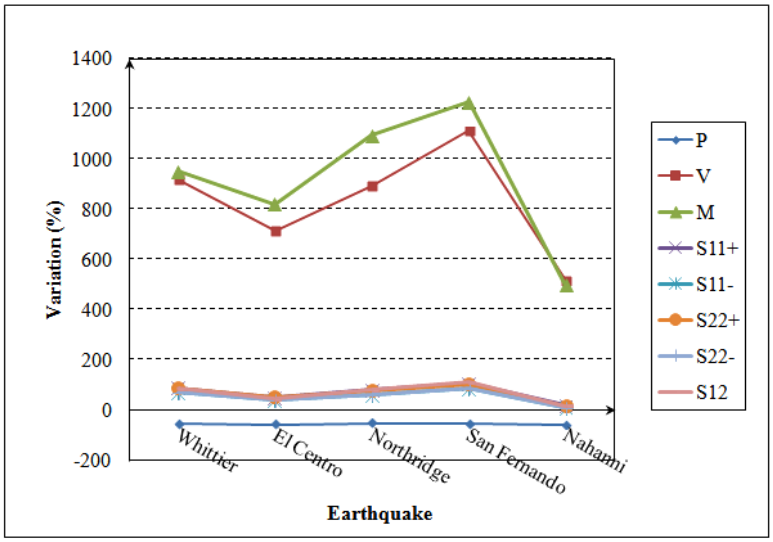

Fig. 9 Variation of pile internal forces and abutment stresses: proposed combination versus
AASHTO 2010 Strength I-contraction mode and class A

4.2. Effects of earthquake intensity

The earthquake forces depend on the site soil condition. As noted previously, results given were for site class 'D' of AASHTO 2010. If we change the site class to 'A' the seismic forces reduce due to a decrease in the scale factor used in time history analyses (see Table 1). The results for this site class are shown in Figs. 9-12. The maximum change is 10% for the Nahanni earthquake.

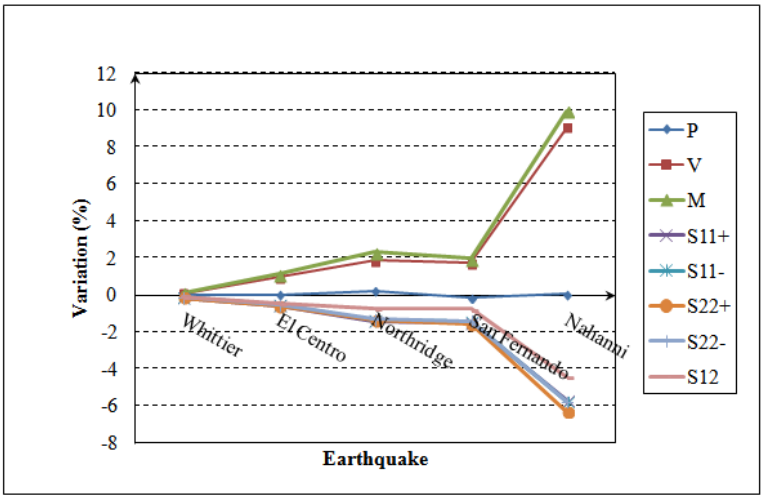

Fig. 10 Variation of pile internal forces and abutment stresses: proposed combination versus
AASHTO 2010 Extreme Event I -contraction mode and class A

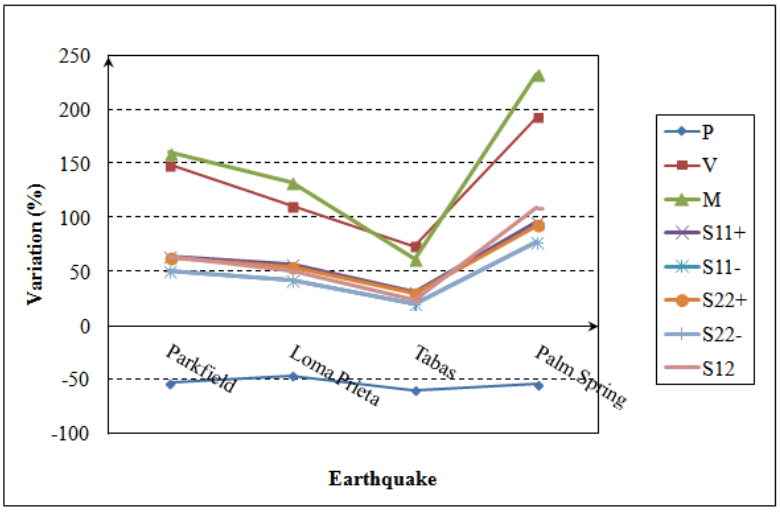

Fig. 11 Variation of pile internal forces and abutment stresses: proposed combination versus
AASHTO 2010 Strength I-expansion mode and class A

Many existing IABs perhaps were not designed by AASHTO (2010). In this code, the design earthquake is an earthquake with a return period of 1000 years. Previous edition of AASHTO (2007) considered a return period of 475 years for the design earthquake. This also reduces the earthquake forces and the corresponding scale factors (see Table 1) for time history analyses. Figs. 13-14 show the analyses results for the same earthquakes and load combinations based on the AASHTO (2007) seismic forces in controlling contraction mode. It is seen that a maximum change of 11% in actions occurs in contraction mode for pile moment in Nahanni earthquake. In

other words, when the actual temperature of an earthquake is considered in the analysis the pile moment increases by 11% compared to the case when earthquake alone is acting.

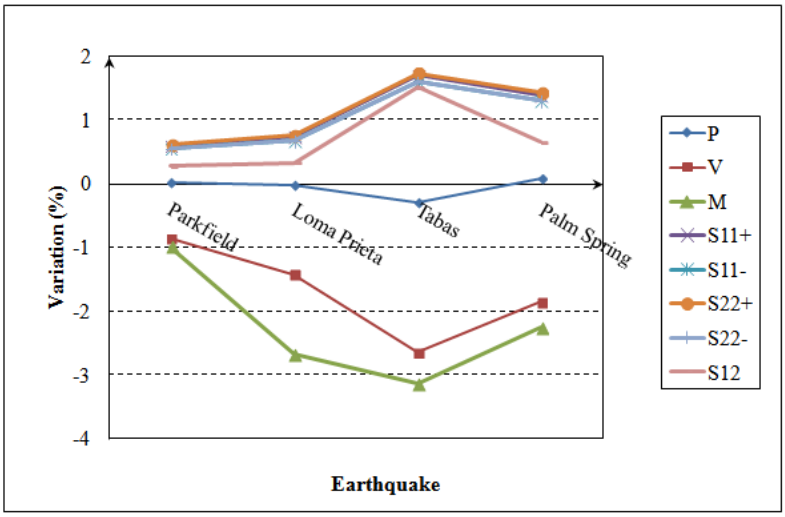

Fig. 12 Variation of pile internal forces and abutment stresses: proposed combination versus
AASHTO 2010 Extreme Event I-expansion mode and class A

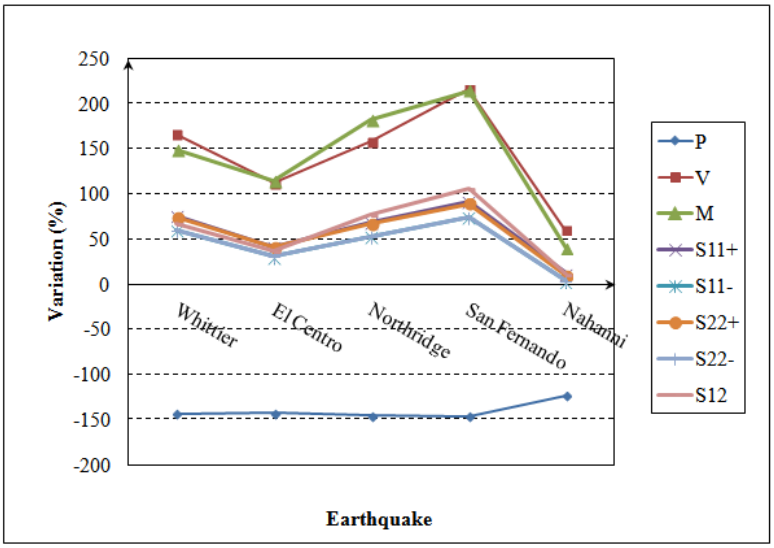

Fig. 13 Variation of pile internal forces and abutment stresses: proposed combination versus
AASHTO 2007 Strength I-contraction mode-Soil type II

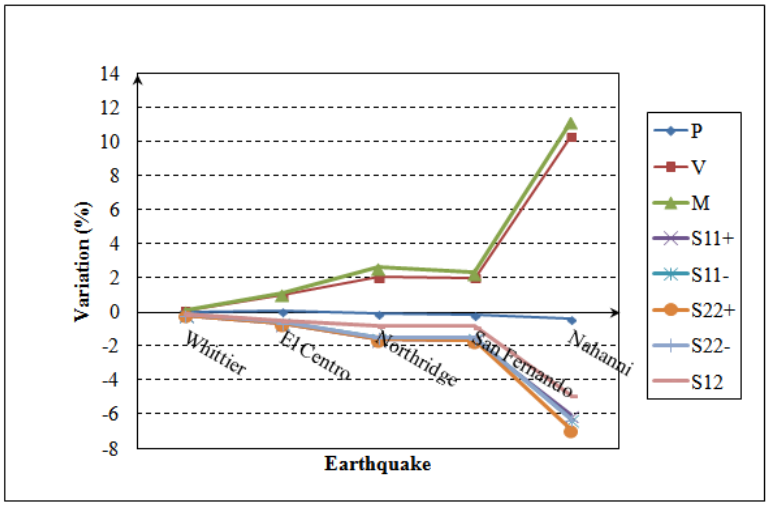

Fig. 14 Variation of pile internal forces and abutment stresses: proposed combination versus
AASHTO 2007 Extreme Event I-contraction mode-Soil type II

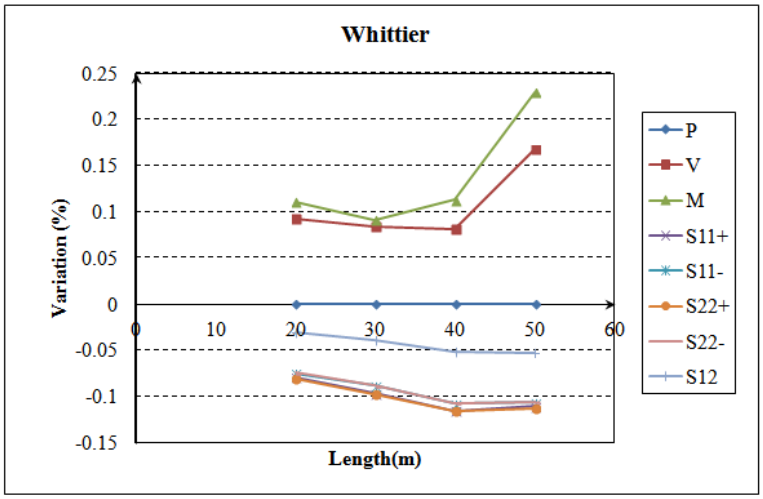

Fig. 15 Variation of pile internal forces and abutment stresses vs. span length: proposed combination versus AASHTO Extreme Event I for Whittier with $\Delta T = -1^{o}C$ (Class D)

4.3. Effects of span length

Next, the IAB spans are varied from 20 to 50 m in 10 m increments. Span length is a major parameter affecting both earthquake and thermal loadings of integral bridges. The variation of pile internal forces and abutment stresses under the EE+T combination is compared with AASHTO's EE-1 for each earthquake case in Figs. 15-19. Results for the expansion mode is of little significance and therefore not shown. The following conclusions can be made:

a) The temperature effects for abutment stresses and piles axial forces are negligible. Piles shears and moments are affected the most by the temperature change that accompanies an earthquake.
b) In general, the temperature effects increase as the span length increases. However, earthquake loading depends on the span length or the longitudinal natural frequency of the structure as well. Therefore, when this is close to the frequency content of the ground motion responses increase.

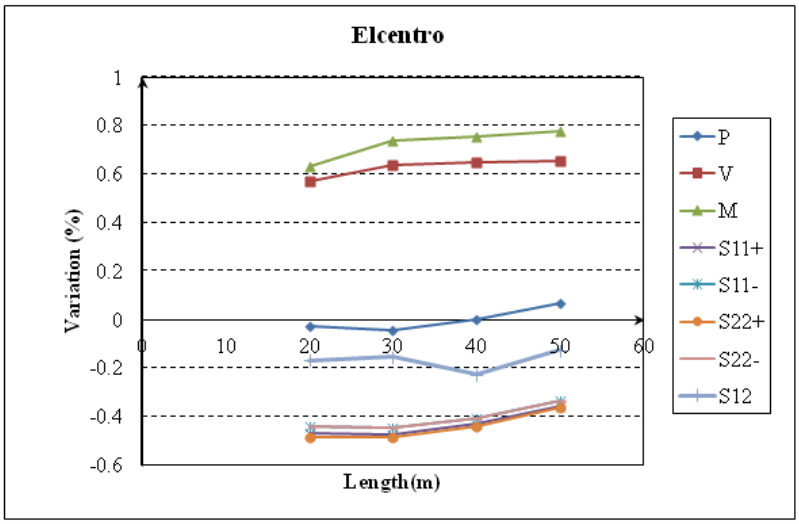

Fig. 16 Variation of pile internal forces and abutment stresses vs. span length: proposed combination versus AASHTO Extreme event I for El Centro withΔT= - 4^{o}C (Class D)

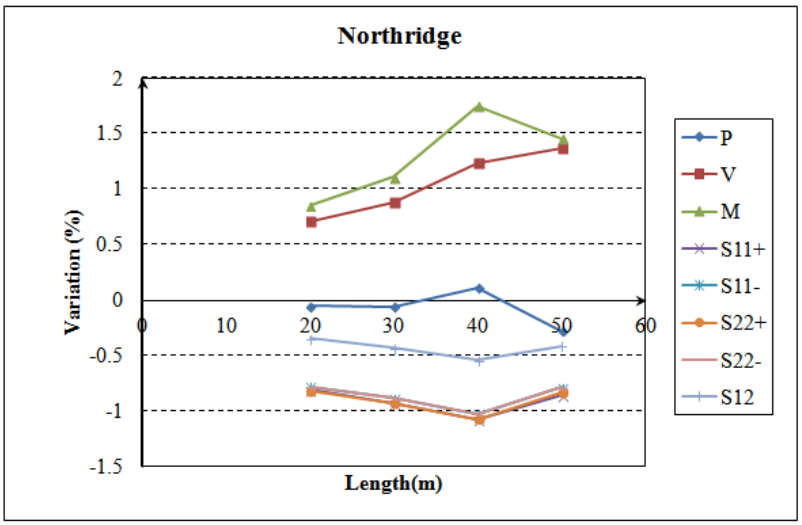

Fig. 17 Variation of pile internal forces and abutment stresses vs. span length: proposed combination versus AASHTO Extreme event I for Northridge with ΔT= - 10^{o}C (Class D)

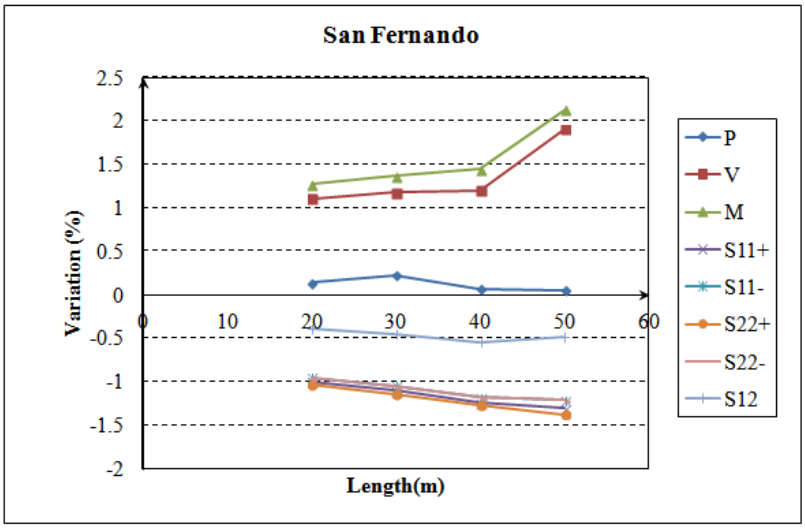

Fig. 18 Variation of pile internal forces and abutment stresses vs. span length: proposed combination versus AASHTO Extreme event I for San Fernando with $\Delta T = -14^{o}C$ (Class D)

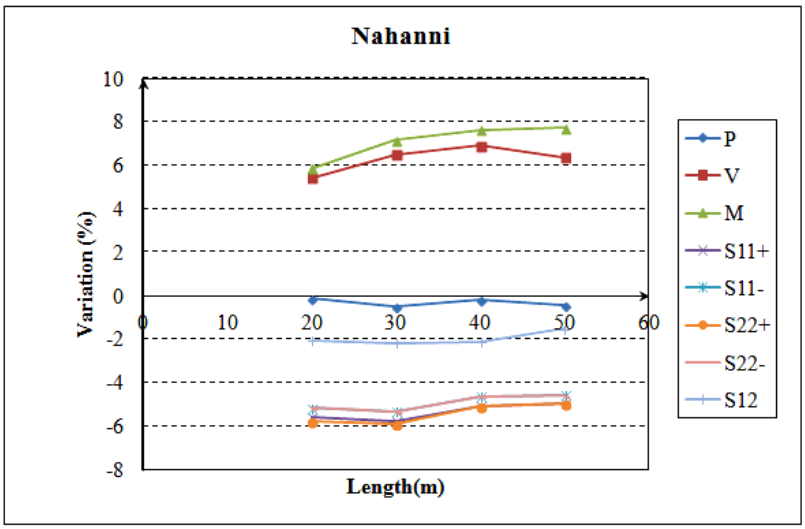

Fig. 19 Variation of pile internal forces and abutment stresses vs. span length: proposed combination versus AASHTO Extreme event I for Nahanni with $\Delta T = -30^{o}C$ (Class D)

4.4. Critical temperature loading

In this section, we intend to find the minimum variation of temperature (ΔT) in the proposed EE+T combination that causes force demands in excess of 10% of AASHTO's EE1 combination for different earthquakes. Both positive and negative temperature changes are considered, but the latter controls in all cases. The results for the earthquakes that cause contraction are shown in Fig. 20. It is seen that the ΔT

ranges from -28 to -45°C for different earthquakes with an average of -36°C. Therefore, it can be concluded that the effects of temperature change accompanying an earthquake can be significant for IABs in cold regions when it is roughly beyond -36°C.

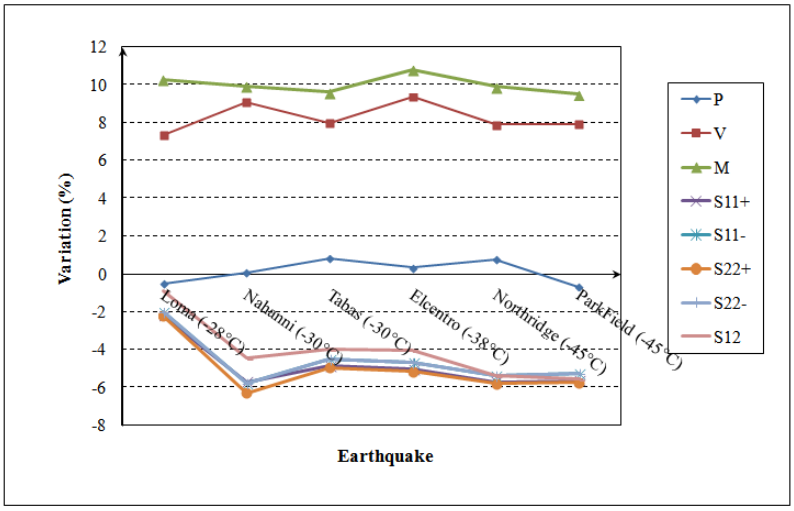

Fig. 20 Variation of pile internal forces and abutment stresses : proposed combination versus AASHTO Extreme Event I for earthquakes with minΔT to achieve a variation of 10%

5. Conclusions

In this paper, the necessity of combining thermal and seismic loads in the design of Integral bridges was investigated. This load combination is not currently required by major bridge design codes. For this purpose, a finite element model that considers nonlinearity in the behavior of near abutment soil in addition to an elastic free field soil response was employed for dynamic time history analyses. The p-y soil response next to piles has been modeled with nonlinear springs. A new load combination (called EE+T) using an estimated temperature change at the time of an earthquake along with the earthquake load was considered in analyses. This load combination was checked against AASHTO's recommended design combinations (S1 & EE1). The following conclusions can be drawn:

- Negative temperature changes causing contraction in IABs are more critical. In other words, the design of IABs in cold earthquake prone regions by current design code regulations could be unsafe. However, for expansion mode the effects of combining seismic and thermal loading can be ignored.
- Parameters like the intensity and frequency content of earthquakes, span length and variation of temperature have been studied. It was found that temperature change is the most important factor affecting the design of IABs.
- Roughly speaking, a design temperature change beyond -36°C is expected to cause changes in piles moments and shears above 10%, indicating an unsafe

structure. For these cases, considering a combined thermal and earthquake loading is recommended.

- Future work can consider a reliability methodology consistent with the AASHTO LRFD design code to arrive at an appropriate load factor for thermal loading in Extreme Event I combination.

References

Bridge Design Specifications (2007), *AASHTO LRFD*, American Association of State Highway and Transportation Officials, AASHTO LRFD Bridge Design Specifications, Washington, D.C.

Bridge Design Specifications (2010), *AASHTO LRFD*, American Association of State Highway and Transportation Officials, AASHTO LRFD Bridge Design Specifications, Washington, D.C.

Comité Européen de Normalisation (CEN) (2008), *Eurocode 8*: Design of structures for earthquake resistance. Part 2: Bridges.

Dicleli M, Albhaisi SM. (2004), "Effect of cyclic thermal loading on the performance of steel H-piles in integral bridges with stub-abutments", *J. Constructional Steel Research*, **60**(2), 161-182.

Duncan JM, Arsoy S. (2003), "Effect of bridge-soil interactions on behavior of piles supporting integral bridges", *Transportation Research Record,* 91-97.

Fennema JL, Lama JA, Linzell DG. (2005), "Predicted and measured response of on integral abutment bridge", *ASCE, J. Bridge Engineering*, **10** (6), 666-677.

Frosch, RJ, Kreger ME, Talbott AM. (2009), *Earthquake Resistance of Integral Abutment Bridges*, Publication FHWA/IN/JTRP-2008/11. Joint Transportation Research Program, Indiana Department of Transportation and Purdue University, West Lafayette, Indiana, doi:10.5703/1288284313448.

Itani A, Pekcan, G. (2011), *Seismic Performance of Steel Plate Girder Bridges with Integral Abutments*, Publication No. FHWA-HIF-11-043.

Kim W, Laman JA. (2010), "Integral abutment bridge response under thermal loading", *Engineering Structures*, **32**, 1495-1508.

Kim W, Laman JA. (2010),"Numerical analysis method for long-term behavior of integral abutment bridges", *Engineering Structures*, **32**, 2247-2257.

Kim W, Laman JA. (2013), "Integral abutment bridge behavior under uncertain thermal and time-dependent load", *Structural Engineering and Mechanics*, **46** (1), 53-73.

Kim W, Laman JA, Park JY. (2014), "Reliability-based design of prestressed concrete girders in integral Abutment Bridges for thermal effects", *Structural Engineering and Mechanics*, **50** (3), 305-322.

Maleki S, Mahjoubi S. (2010), "A new approach for estimating the seismic soil pressure on retaining walls", J.*Scientia Iranica*, **17**(4), 273-284.

PEER Strong Motion Database (2013), http://peer.berkeley.edu/smcat.

Reese LC, Van Impe WF. (2001), *Single Piles and Pile Groups under Lateral Loading*", A.A. Balkema, Rotterdam, Netherlands.

Shah BR. (2007), "3D finite element analysis of integral abutment bridges subjected to thermal loading", M.S. Dissertation, Civil Engineering College of Engineering of

Kansas State University, Manhattan.

Spyrakos C, Loannidis G. (2003), “Seismic behavior of a post-tensioned integral bridge including soil–structure interaction (SSI)”, *Soil Dynamics and Earthquake Engineering*, **23**,53–63.

Tegos I, Sextos A, Mitoulis S, Tsitotas M. (2005), “Contribution to the improvement of seismic performance of integral Bridges”, *Proceedings 4th European Workshop on the Seismic Behavior of Irregular and Complex Structures*, Thessaloniki, Greece.

Tsang NCM, England GL. (2002), “Soil/structure interaction of integral bridge with full height abutments”, *Proceedings of the 15th ASCE Engineering Mechanics Conference*, Columbia University, NY.